JOURNAL OF APPLIED PHYSICS **117**, 093906 (2015)

Strain dependent electron spin dynamics in bulk cubic GaN

A. Schaefer,[1] J. H. Buß,[1] T. Schupp,[2] A. Zado,[2] D. J. As,[2] D. Hägele,[1] and J. Rudolph[1]
[1]*Arbeitsgruppe Spektroskopie der kondensierten Materie, Ruhr-Universität Bochum, Universitätsstraße 150, D-44780 Bochum, Germany*
[2]*Department of Physics, University of Paderborn, Warburger Str. 100, D-33095 Paderborn, Germany*

(Received 14 November 2014; accepted 23 February 2015; published online 5 March 2015)

The electron spin dynamics under variable uniaxial strain is investigated in bulk cubic GaN by time-resolved magneto-optical Kerr-rotation spectroscopy. Spin relaxation is found to be approximately independent of the applied strain, in complete agreement with estimates for Dyakonov-Perel spin relaxation. Our findings clearly exclude strain-induced relaxation as an effective mechanism for spin relaxation in cubic GaN. © *2015 AIP Publishing LLC*.
[http://dx.doi.org/10.1063/1.4914069]

I. INTRODUCTION

Today's semiconductor electronics with its wealth of devices is based on sophisticated control over the orbital motion of electrons, which is accomplished mainly by electric fields acting on the charge of electrons. Substantially new concepts will, however, soon be required as the relevant length scales of conventional, charge-based electronics are continuously shrinking.[1] Spintronics as a spin-based electronics is such an alternative approach, which uses in addition also the spin of electrons and promises improved performance or even new device functionality.[2–5] Most concepts for spintronic devices require that the electron spin can be efficiently manipulated and that an initially prepared non-equilibrium spin polarization is sustained, respectively.[2,6] Both problems are often closely linked to spin-orbit coupling (SOC) for mobile electrons in III–V semiconductors, where typically strong SOC is desired for efficient spin manipulation, while weak SOC permits long spin lifetimes. One approach to adjust the strength of SOC are external fields, where, e.g., electric fields allow for an efficient electron spin manipulation via the Rashba effect,[7] but also influence electron spin relaxation.[8–10] Strain fields are another attractive handle to tune SOC as they can be permanently introduced by, e.g., strain engineering in semiconductor heterostructures,[11–14] flexibly applied by external mechanical forces[15–18] or even dynamically modulated at high frequencies.[19] Strain fields applied in such ways can significantly modify spin dynamics.[17,18,20–24] Aiming at slow spin relaxation, semiconductors with intrinsically weak SOC are another promising approach. Especially GaN is expected to offer long spin lifetimes due to its combination of weak SOC and large band gap.[25] Slow spin relaxation was indeed observed in the metastable cubic phase of GaN (c-GaN) with its high symmetry,[26,27] while the thermodynamically favored hexagonal phase of GaN (h-GaN) shows fast spin relaxation due to its lower symmetry.[28–30] The experimental spin relaxation times in c-GaN are, however, still substantially shorter than theoretically predicted.[31] Unintentional strain fields caused by microstrain variations[32–34] or by a small h-GaN content[35] were discussed as a possible reason for the observed discrepancy.[27] The impact of strain fields on spin relaxation in c-GaN has, however, not been studied so far. Here, we investigate the electron spin dynamics in bulk c-GaN under variable uniaxial strain by time-resolved magneto-optical Kerr-rotation (TRKR) spectroscopy.

II. EXPERIMENTAL

The c-GaN samples were grown by plasma assisted molecular beam epitaxy.[36] Sample A consists of a 400 nm-thick c-GaN layer grown on top of a 30 nm-thick 3C-SiC layer on Si(001) substrate, resulting in a low n-type doping of the c-GaN layer with a carrier density of $n_D = 6 \times 10^{16}\,\mathrm{cm}^{-3}$. For sample B, an intentionally undoped 570 nm-thick c-GaN layer was deposited on 30 nm cubic AlN on top of a 10 μm-thick 3 C-SiC layer on Si(001) substrate, leading to an n-type doping density of $n_D = 1 \times 10^{17}\,\mathrm{cm}^{-3}$ of the top c-GaN. The Si substrates of both samples were afterwards mechanically polished down to a thickness of approximately 100 μm for the strain dependent measurements. The thinned samples were glued[37] on stacked $PbZrTiO_3$ (PZT) piezoelectric actuators[38] with the $\langle 110 \rangle$ direction along the poling direction of the piezo stack, following the approach of Ref. 39. The applied strain was continuously monitored via resistive strain gauges[40] glued to the back of the piezo stacks. The strain transmitted to the samples was additionally checked by strain gauges glued on top of the samples.[41]

For the TRKR measurements, the output of a fs-mode-locked Ti:sapphire laser was frequency-doubled and split into pump and probe beam. The polarization of the pump beam was modulated between right and left circularly polarized by a photo-elastic modulator with a modulation frequency of 50 kHz. The pump beam was afterwards focused down to a spot with a diameter of approximately 100 μm on the samples surface, exciting electrons with a temporally varying electron spin polarization corresponding to the modulated polarization of the pump beam. The spin dynamics of the electron ensemble was monitored via the Kerr-rotation of the linearly polarized probe beam as a function of the time delay between pump and probe pulses, which was varied by a mechanical delay line. The Kerr-rotation was detected via a balanced receiver and a cascaded lock-in scheme, using the high frequency polarization modulation of

0021-8979/2015/117(9)/093906/7/$30.00

the pump beam as the first reference and an intensity modulation of the probe beam via a mechanical chopper at a much lower frequency of about 0.6 kHz as the second reference. The energy of pump and probe beam was set to the maximum of the TRKR signal at 3.21 eV, and the average pump and probe power were $P_{\text{pump}} = 8$ mW and $P_{\text{probe}} = 0.8$ mW, respectively, for sample A and $P_{\text{pump}} = 10$ mW and $P_{\text{probe}} = 1$ mW, respectively, for sample B. An external magnetic field B_{ext} was applied in the sample plane. All measurements were carried out at room-temperature.

III. RESULTS AND DISCUSSION

Figure 1 shows typical TRKR transients of sample A for zero strain and maximum applied strain, respectively, in an external magnetic field $B_{\text{ext}} = 0.13$ T. The oscillations of the TRKR signal are caused by spin Larmor precession with frequency ω_L around the external magnetic field, while the temporal decay of the TRKR signal amplitude directly reflects spin relaxation. The almost perfect match of the transients in Fig. 1 already indicates an only minute influence of the applied strain both on spin precession and spin relaxation. The Larmor precession frequency ω_L and the spin relaxation time τ_s are obtained by damped cosine fits of the form[29] $[A_1 \exp(-t/\tau_c) + A_2] \exp(-t/\tau_s) \cos[\omega_L(t - t_0)]$ to the TRKR transients. Figure 2 shows the corresponding Landé g_e-factor $g_e = \hbar\omega_L/\mu_B B_{\text{ext}}$ as a function of the applied strain. The zero-strain value of g_e is in very good agreement with the literature value of 1.95 for electrons in c-GaN.[42,43] The g_e-factor shows only a negligible strain dependence, which is expected[44,45] for the wide-gap GaN, and which further demonstrates the weak SOC in GaN.

In the following, we will discuss the strain dependence of the spin relaxation time τ_s as the main point of this work. Figure 3 shows τ_s as a function of the applied strain for both samples. The value of the spin relaxation time is for each applied strain averaged over at least five measurements, where the strain has been varied in a non-monotonic way in between the measurements to minimize spurious effects due to possible drifts in the setup. The spin relaxation time shows no distinct strain dependence within the experimental uncertainty. We note that comparable strain values already lead to a substantial decrease of spin lifetimes in, e.g., GaAs.[17,20–23] In the following, we will compare the observed negligible strain dependence of spin relaxation to theoretical predictions.

Spin relaxation of free, delocalized conduction band electrons is usually governed by Dyakonov-Perel (DP) spin relaxation[46] in bulk III–V semiconductors.[10,47] DP relaxation is driven by the combined action of an intrinsic conduction band spin splitting and random momentum scattering: the spin splitting acts like a wavevector dependent, effective magnetic field $\mathbf{\Omega}(\mathbf{k})$ on the electrons' spins, leading to spin precession. Random momentum scattering results in

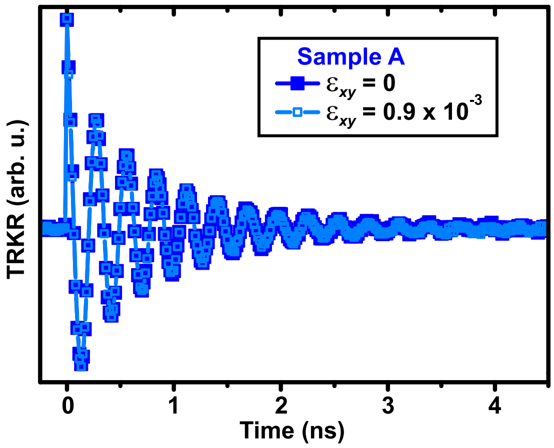

FIG. 1. TRKR transients for sample A for zero strain and maximum applied strain ϵ_{xy} in an external magnetic field $B_{\text{ext}} = 0.13$ T.

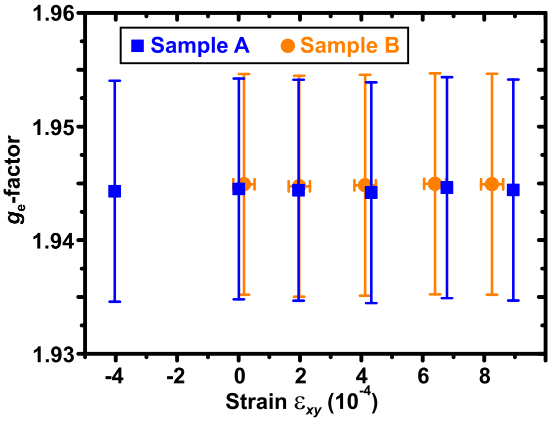

FIG. 2. Room temperature strain dependence of the Landé g_e-factor for sample A and B.

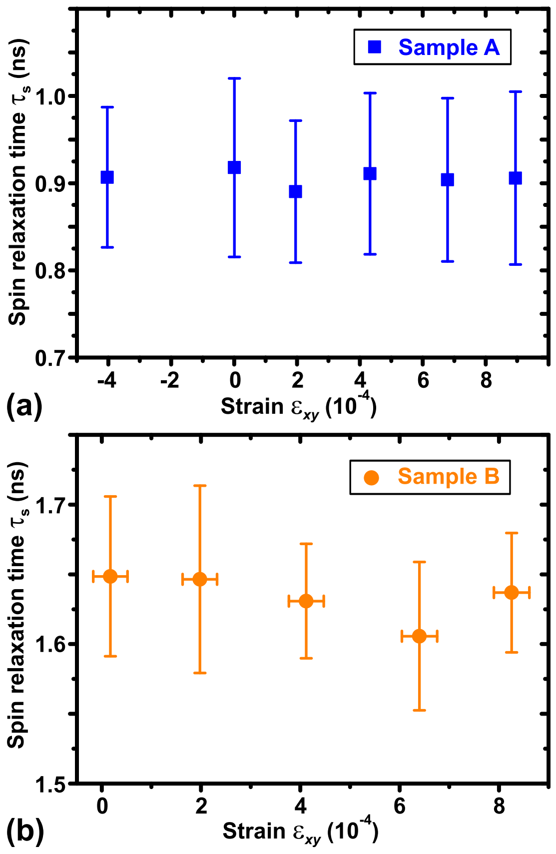

FIG. 3. Spin relaxation time τ_s as a function of the applied strain ϵ_{xy} for (a) sample A and (b) sample B at room-temperature.

fluctuations of this effective magnetic field, causing in the end spin dephasing of an electron ensemble. Formally, the action of the effective magnetic field is described by the Hamiltonian

$$H_{\text{so}} = \frac{\hbar}{2}\mathbf{\Omega}(\mathbf{k}) \cdot \boldsymbol{\sigma} \tag{1}$$

with $\boldsymbol{\sigma}$ as the vector of Pauli spin matrices, which further illustrates the interpretation of $\mathbf{\Omega}(\mathbf{k})$ as an effective magnetic field by the formal correspondence to the Hamiltonian of the Zeeman effect. In uniaxially strained bulk cubic crystals, two terms contribute to the conduction band spin splitting, corresponding to the total effective magnetic field

$$\mathbf{\Omega}_{\text{total}}(\mathbf{k}) = \mathbf{\Omega}_{\text{D}}(\mathbf{k}) + \mathbf{\Omega}_{\text{str}}(\mathbf{k}). \tag{2}$$

The so-called Dresselhaus term[48]

$$\mathbf{\Omega}_{\text{D}}(\mathbf{k}) = \frac{2\gamma_e}{\hbar}\begin{pmatrix} k_x(k_y^2 - k_z^2) \\ k_y(k_z^2 - k_x^2) \\ k_z(k_x^2 - k_y^2) \end{pmatrix} \tag{3}$$

with γ_e as the spin splitting constant stems from the intrinsic bulk inversion asymmetry of semiconductors with zinc-blende structure. Uniaxial strain leads in lowest order (that is linear in k and ϵ) to the second term[20–23]

$$\mathbf{\Omega}_{\text{str}}(\mathbf{k}) = (C_3\phi + C_3'\psi)/\hbar, \tag{4}$$

where

$$\phi_i = \epsilon_{i+1,i}k_{i+1} - \epsilon_{i+2,i}k_{i+2} \tag{5}$$

and

$$\psi_i = k_i(\epsilon_{i+1,i+1} - \epsilon_{i+2,i+2}) \tag{6}$$

with $i = x,y,z$ and ϵ_{ij} as components of the strain tensor ϵ. Accordingly, the material dependent parameters C_3 and C_3' govern the size of the strain-induced spin splitting. Usually, $C_3 \gg C_3'$ is assumed as C_3' vanishes in a three-band model and appears only upon inclusion of higher conduction band states.[20,22,49] In agreement with $C_3 \gg C_3'$, experiments in GaAs and GaSb [21–23] showed increasing spin relaxation rates for uniaxial strain along the $\langle 111\rangle$ and $\langle 110\rangle$ directions, respectively, while the spin relaxation rate was independent of the strain for uniaxial strain along the $\langle 100\rangle$ direction, where the strain tensor ϵ is diagonal. In the following, we will therefore only consider the term $C_3\phi$ in Eq. (4), though more recent calculations suggest that C_3 and C_3' could be comparable in size.[50]

For the case investigated here with uniaxial strain along the $\langle 110\rangle$ direction, the only non-zero off-diagonal components of the strain tensor ϵ are $\epsilon_{xy} = \epsilon_{yx}$, and the effective magnetic field reduces to

$$\mathbf{\Omega}_{\text{str}}^{\langle 110\rangle}(\mathbf{k}) = \frac{C_3}{\hbar}\begin{pmatrix} \epsilon_{xy}k_y \\ -\epsilon_{xy}k_x \\ 0 \end{pmatrix}. \tag{7}$$

In the most simplistic form of DP theory, the tensor of spin relaxation rates γ_{ij} follows from the effective magnetic field by[51]

$$\gamma_{ij} = \frac{1}{2}\left(\delta_{ij}\langle\overline{\mathbf{\Omega}^2}\rangle - \langle\overline{\Omega_i\Omega_j}\rangle\right)\tau_p, \tag{8}$$

where the overbar denotes the angular average over $\mathbf{k}$, $\langle\ldots\rangle$ denotes the energetic average over the electronic momentum distribution and τ_p is the effective, averaged momentum scattering time. A more accurate description accounts, however, for the energy dependence and efficiency of individual momentum scattering processes by the tensor of energy dependent spin relaxation rates[25]

$$\tilde{\gamma}_{ij} = \left(\delta_{ij}\overline{\mathbf{\Omega}^2} - \overline{\Omega_i\Omega_j}\right)\left(\sum_\nu \frac{\gamma_\ell^\nu}{\tilde{\tau}_p^\nu}\right)^{-1}, \tag{9}$$

where the summation runs over the different momentum scattering mechanisms. The efficiency factors γ_ℓ depend on the nature of $\mathbf{\Omega}(\mathbf{k})$ and the individual momentum scattering process.[5,47,52] The final spin relaxation rates γ_{ij} are obtained by energetically averaging over the electronic momentum distribution. Here, we approximate the electronic momentum distribution by a Boltzmann distribution as the Fermi temperatures $T_F^A = E_F^A/k_B = 43\,\text{K}$ for sample A and $T_F^B = 61\,\text{K}$ for sample B, respectively, with $E_F = (3\pi^2)^{2/3}\hbar^2 n_D^{2/3}/2m^*$ as the Fermi energy are well below the lattice temperature of 293 K for both samples. A total spin relaxation rate

$$\gamma_{ij}^{\text{total}} = \gamma_{ij}^{\text{D}} + \gamma_{ij}^{\text{str}} \tag{10}$$

follows accordingly for the total effective magnetic field $\mathbf{\Omega}_{\text{total}}(\mathbf{k})$ of Eq. (2). We note that here no interference of the Dresselhaus and the strain term occurs, unlike the case of bulk wurtzite GaN[29] or two-dimensional electron systems with both Dresselhaus and Rashba term.[53] Spin relaxation due to the Dresselhaus term with the effective magnetic field $\mathbf{\Omega}_{\text{D}}(\mathbf{k})$ according to Eq. (3) is isotropic with a rate

$$\gamma_s^{\text{D}} = \frac{1}{\tau_s^{\text{D}}} = \frac{8\gamma_e^2 m^{*3}}{\hbar^8}(k_BT)^3\left(\sum_i \frac{1}{Q_i\tau_p^i}\right)^{-1} \tag{11}$$

and the averaged momentum scattering time $\tau_p^i = \langle\tilde{\tau}_p^i E_k\rangle/\langle E_k\rangle$. The efficiency coefficients

$$Q_i = \frac{32}{105}\frac{1}{\gamma_3^i}\frac{\langle\tilde{\tau}_p^i E_k^3\rangle\langle E_k\rangle}{\langle\tilde{\tau}_p^i E_k^3\rangle(k_BT)^3} = \frac{16}{35}\frac{\left(\nu + \frac{7}{2}\right)\left(\nu + \frac{5}{2}\right)}{\gamma_3^i} \tag{12}$$

are introduced for γ_ℓ with $\ell = 3$ for the cubic k^3-Dresselhaus term[47,52] and assuming a power law $\tilde{\tau}_p \propto E_k^\nu$ for the individual scattering mechanisms.

The second term in Eq. (2) with the strain induced effective magnetic field $\mathbf{\Omega}_{\text{str}}^{\langle 110\rangle}(\mathbf{k})$ leads to anisotropic spin relaxation with rates

$$\gamma_{zz}^{\text{str}} = 2\gamma_{xx}^{\text{str}} = 2\gamma_{yy}^{\text{str}} = \frac{2C_3^2 m^* k_BT}{\hbar^4}\epsilon_{xy}^2\tau_p^{\text{total}}. \tag{13}$$

The efficiency factors γ_ℓ simplify in this case to $\gamma_1 = 1$ with $\ell = 1$ for the linear-in-k effective magnetic field $\mathbf{\Omega}_{\text{str}}^{\langle 110\rangle}(\mathbf{k})$,[47,52] resulting in

$$\tau_p^{\text{total}} = \left(\sum_i \frac{1}{\tau_p^i}\right)^{-1}. \tag{14}$$

The application of an external magnetic field B_{ext} in the xy-plane as in the experiment leads to spin Larmor precession around B_{ext} and the observation of an averaged effective spin relaxation rate[28,54]

$$\gamma_{\text{eff}}^{\text{str}} = 1/\tau_{s,\text{eff}}^{\text{str}} = (\gamma_{zz}^{\text{str}} + \gamma_{xx}^{\text{str}})/2, \tag{15}$$

giving

$$\gamma_{\text{eff}}^{\text{str}} = \frac{3}{4}\gamma_{zz}^{\text{str}} = \frac{3}{2}\frac{C_3^2 m^* k_B T}{\hbar^4}\epsilon_{xy}^2 \tau_p^{\text{total}} \tag{16}$$

for $\gamma_{zz}^{\text{str}} = 2\gamma_{xx}^{\text{str}}$ according to Eq. (13).

For a quantitative comparison of the experimental spin relaxation rate and its strain dependence to the predictions of DP theory, the spin splitting constant γ_e, the strain spin splitting constant C_3 and the momentum scattering times τ_p^i have to be known. The spin splitting constant γ_e in c-GaN has only been theoretically predicted by few tight-binding calculations,[26,55–57] resulting in values between $\gamma_e = 0.235\,\text{eV}\,\text{Å}^3$ and $\gamma_e = 0.84\,\text{eV}\,\text{Å}^3$, while no experimental values are available. As the strain spin splitting constant C_3 is not known for c-GaN, we estimate its value via expressions derived within $k \cdot p$-theory,[20,25,49,58] giving in lowest order

$$C_3 = \frac{4}{3}C_2\frac{\hbar P}{m^*}\frac{\eta}{E_g} \approx \frac{4}{3}\hbar C_2 \eta\left[2m^* E_g\left(1 - \frac{1}{3}\eta\right)\right]^{-1/2} \tag{17}$$

with $\eta = \Delta_{so}/(E_g + \Delta_{so})$, Δ_{so} as the split-off energy, and P as the Kane matrix element. While the band parameters m^*, E_g and Δ_{so} are well known,[59,60] the value of the interband deformation potential C_2 is not available for c-GaN. We assume, however, a value between 1 eV and 6 eV for C_2 in the following, as all published values for C_2 in various other semiconductors universally fall in this range (cf. Table I). The strain splitting constant C_3 for c-GaN is then estimated to be between $0.02\,\text{eV}\,\text{Å}$ and $0.11\,\text{eV}\,\text{Å}$ according to Eq. (17). We note that C_3 is about two orders of magnitude smaller in c-GaN than in GaAs[16] as a consequence of the combination of large m^*, large E_g, and small Δ_{so} in c-GaN.

The momentum scattering times τ_p^i are modeled via the corresponding transport mobilities $\mu_i^{\text{sim}} = (e/m^*)\tau_p^i$, as the direct experimental determination of mobilities by transport measurements is hindered by highly conductive substrates. The simulated mobility $\mu_{\text{total}}^{\text{sim}} = (e/m^*)\tau_p^{\text{total}}$ with τ_p^{total} according to Eq. (14) combines scattering by dislocations, polar optical phonons, and ionized impurities as well as piezoelectric scattering and acoustic phonon deformation potential scattering[61–65] via Matthiessen's rule $1/\mu_{\text{total}}^{\text{sim}} = \sum_i 1/\mu_i$, and is overall in good agreement with available experimental values for the mobility in c-GaN.[32,66,67] Figure 4 shows $\mu_{\text{total}}^{\text{sim}}$ in dependence on the dislocation density n_{Disl} as the sample-dependent key parameter for the mobility at room-temperature. Typical dislocation densities are approximately $10^{10}\,\text{cm}^{-2}$ to $10^{11}\,\text{cm}^{-2}$ for sample A, which was grown on a thin SiC layer prepared by carbonizing the Si substrate,[68] while typical dislocation densities for sample B are in the range of $2\times10^9\,\text{cm}^{-2}$–$2\times10^{10}\,\text{cm}^{-2}$ for its epilayer thickness of 570 nm.[69] The total mobility $\mu_{\text{total}}^{\text{sim}}$ is accordingly in the range of $10\,\text{cm}^2/\text{Vs}$–$200\,\text{cm}^2/\text{Vs}$ (cf. Fig. 4).

For the momentum scattering times $Q_i\tau_p^i$, which are weighted by the efficiency coefficients Q_i according to Eqs. (11) and (12) for the cubic Dresselhaus term, only scattering by dislocations and by polar optical phonons is considered, as these two mechanisms dominate by far the room-temperature mobility in c-GaN.[66] The corresponding efficiency factors and efficiency coefficients are $\gamma_3^{\text{disl}} = 6$ and $Q_{\text{disl}} = 32/21$,[70] respectively, for scattering by dislocations, and $\gamma_3^{\text{pop}} = 11/6$ and $Q_{\text{pop}} = 1152/385 \approx 3$, respectively, for scattering by polar optical phonons.[71] Using these values, we will first discuss the spin relaxation rate γ_s^{D} predicted by Eq. (11) for only the Dresselhaus contribution to DP relaxation, i.e., the case of zero strain. Eq. (11) predicts a significantly smaller spin relaxation rate $\gamma_s^{\text{D}} \approx 0.02\,\text{ns}^{-1}$ for sample A and $\gamma_s^{\text{D}} \approx 0.07\,\text{ns}^{-1}$ for sample B, respectively, than observed in the experiment.[72] This discrepancy can originate from two sources: either from an underestimation of spin relaxation

TABLE I. Values of the interband deformation potential C_2 for various semiconductors.

Material	C_2 (eV)	Reference	Remark
GaAs	1.1	58	$C_2 = 2d^{v,cs}$, pseudopotential
	5.5	58	$C_2 = 2d^{v,cs}$, LCAO
	3.0	20	Deduced from experimental value for C_3
GaSb	1.38	58	$C_2 = 2d^{v,cs}$, pseudopotential
	4.4	58	$C_2 = 2d^{v,cs}$, LCAO
	2.2	20	Deduced from experimental value for C_3
InP	2.2	58	$C_2 = 2d^{v,cs}$, pseudopotential
	5.2	58	$C_2 = 2d^{v,cs}$, LCAO
	6.6	20	Deduced from experimental value for C_3
InSb	2.48	58	$C_2 = 2d^{v,cs}$, pseudopotential
	4.50	58	$C_2 = 2d^{v,cs}$, LCAO
	1.0	20	Experimental value

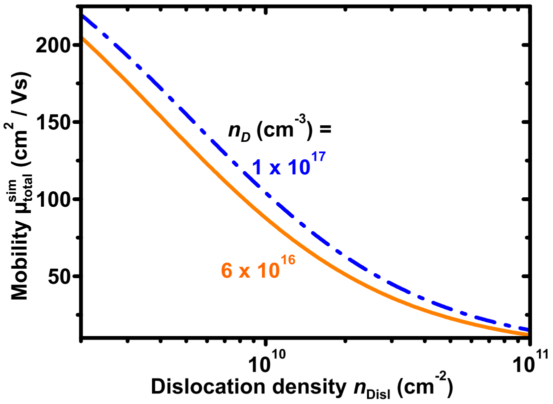

FIG. 4. Simulated transport mobility $\mu_{\text{total}}^{\text{sim}}$ as a function of the dislocation density n_{Disl} for doping densities $n_D = 6\times10^{16}\,\text{cm}^{-3}$ and $n_D = 1\times10^{17}\,\text{cm}^{-3}$, respectively.

within the DP mechanism, or from significant contributions of other spin relaxation mechanisms. Larger DP spin relaxation rates would obviously follow for a larger spin splitting constant γ_e. We note that no experimental value for γ_e is available for c-GaN and that the theoretical prediction of γ_e is notoriously difficult, as is well-known even for deeply studied semiconductors like GaAs. Additional sources of spin splittings would also cause a speed-up of DP relaxation. Such additional spin splittings could originate from the omnipresent inclusions of polar hexagonal GaN in the c-GaN matrix,[33] where the polar faces of the hexagonal GaN inclusions might act like a random Rashba field comparable to the random Rashba fields of dopant ions.[73,74] Furthermore, thermally activated carrier scattering between the cubic and the hexagonal GaN phases could lead to strongly enhanced spin relaxation due to the very fast spin relaxation in the polar hexagonal GaN.[27–30]

Generally, several other spin relaxation mechanisms will also contribute to spin relaxation in c-GaN. Elliott-Yafet[75] (EY) relaxation as well as relaxation due to the Bir-Aronov-Pikus[76] (BAP) mechanism as other spin relaxation mechanisms for mobile electrons[47] are, however, expected to contribute only weakly to spin relaxation. The spin relaxation time due to EY relaxation is estimated to be on the order of μs in c-GaN by expressions for the long-range part,[47,64] and BAP is generally found to be ineffective for n-type samples at high temperatures.[10,47] Instead, the spin relaxation via hyperfine interaction with lattice nuclei[77] of electrons deeply localized at defect or donor states with activation energies on the order of several hundred meV as found in c-GaN[66] might contribute significantly to spin relaxation, where efficient spin exchange between localized and mobile electrons leads to spin relaxation also for the system of delocalized electrons.[78]

In the remaining, we will discuss whether the strain dependence of spin relaxation predicted by DP theory is compatible with the observed negligible strain dependence. Therefore, we simulate the strain dependence of the spin relaxation rate due to DP relaxation, using the above estimates for the strain splitting constant C_3 and for the mobility $\mu_{\mathrm{total}}^{\mathrm{sim}}$. Figure 5 shows the effective spin relaxation rate $\gamma_{\mathrm{eff}}^{\mathrm{str}}$ according to Eq. (16) as a function of the squared strain ϵ_{xy}^2 for different values of the interband deformation potential C_2 and the transport mobility $\mu_{\mathrm{sim}}^{\mathrm{total}}$. Overall, the strain-induced spin relaxation rate is well below 1 $\mu\mathrm{s}^{-1}$ for the investigated strain range even for the extreme combination of the maximum estimated values for both C_2 and the mobility. Thus, a very weak contribution of strain-induced DP relaxation to the total electron spin relaxation is predicted for c-GaN. For further comparison to the experiment, we add the experimental zero-strain spin relaxation rate $\gamma_s^{\mathrm{exp}}(\epsilon_{xy}=0)$ to the predicted strain-dependent rate $\gamma_{\mathrm{eff}}^{\mathrm{str}}$ to account for other spin relaxation mechanisms, and plot the resulting total rate $\gamma_s^{\mathrm{total}} = \gamma_s^{\mathrm{exp}}(\epsilon_{xy}=0) + \gamma_{\mathrm{eff}}^{\mathrm{str}}$ (solid lines in Fig. 6) together with the experimental spin relaxation rates $\gamma_s = 1/\tau_s$ (symbols in Fig. 6) versus the squared strain. The very good agreement apparent from Fig. 6 clearly excludes strain-induced contributions to DP spin relaxation as an efficient spin relaxation mechanism in c-GaN.

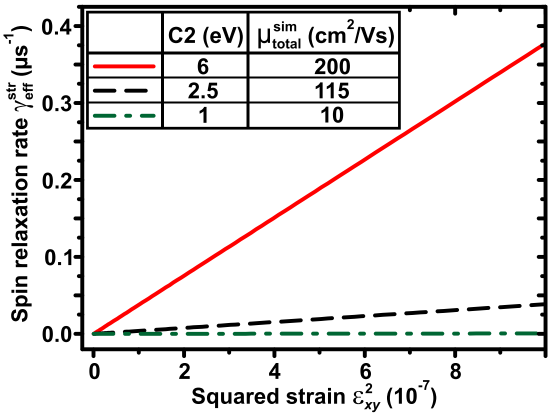

FIG. 5. Simulated strain dependence of the strain-induced spin relaxation rate $\gamma_{\mathrm{eff}}^{\mathrm{str}}$ for different values of the interband deformation potential C_2 and mobility $\mu_{\mathrm{total}}^{\mathrm{sim}}$.

IV. CONCLUSION

In conclusion, we have experimentally investigated the strain dependence of electron spin dynamics in bulk cubic GaN. A negligible strain dependence of spin relaxation is found, which is shown to be completely compatible with Dyakonov-Perel theory, while the spin relaxation rates for zero strain are strongly underestimated by Dyakonov-Perel theory. Possible reasons for this discrepancy are discussed.

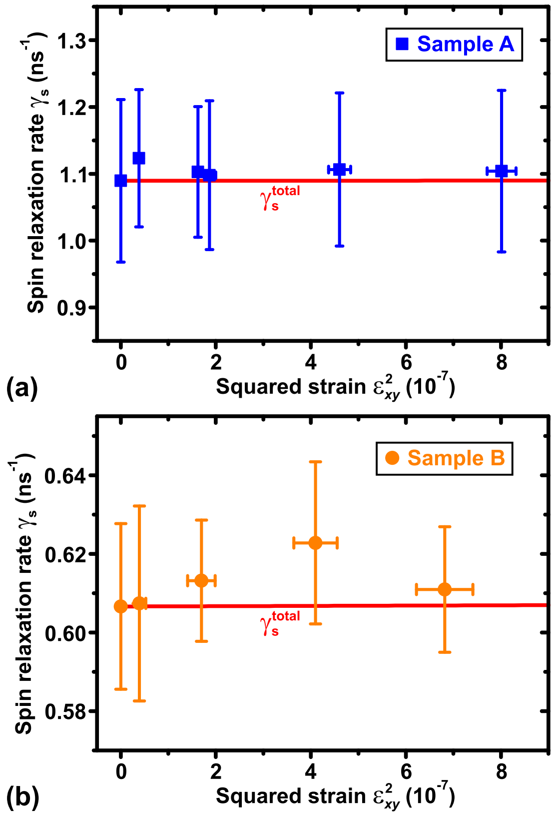

FIG. 6. Experimental spin relaxation rate γ_s (symbols) as a function of the squared strain ϵ_{xy}^2 for (a) sample A and (b) sample B. The solid lines show the strain dependence predicted by Dyakonov-Perel theory for $C_2 = 6\,\mathrm{eV}$ and $\mu_{\mathrm{sim}}^{\mathrm{total}} = 200\,\mathrm{cm}^2/\mathrm{Vs}$.

ACKNOWLEDGMENTS

We gratefully acknowledge financial support by the German Science Foundation (DFG priority program 1285 "Semiconductor Spintronics" and DFG graduate program GRK 1464 "Micro- and Nanostructures in Optoelectronics and Photonics").

[1] S. E. Thompson and S. Parthasarathy, Mater. Today **9**, 20 (2006).

[2] S. A. Wolf, D. D. Awschalom, R. A. Buhrman, J. M. Daughton, S. von Molnár, M. L. Roukes, A. Y. Chtchelkanova, and D. M. Treger, Science **294**, 1488 (2001).

[3] *Semiconductor Spintronics and Quantum Computation*, edited by D. D. Awschalom and N. Samarth (Springer-Verlag, Berlin, 2002).

[4] *Spin Physics in Semiconductors*, edited by M. I. Dyakonov (Springer-Verlag, Berlin, 2008).

[5] I. Zutic, J. Fabian, and S. D. Sarma, Rev. Mod. Phys. **76**, 323 (2004).

[6] D. D. Awschalom and M. E. Flatté, Nat. Phys. **3**, 153 (2007).

[7] E. I. Rashba, Sov. Phys. Solid State **2**, 1109 (1960).

[8] M. Furis, D. L. Smith, S. A. Crooker, and J. L. Reno, Appl. Phys. Lett. **89**, 102102 (2006).

[9] A. Balocchi, Q. H. Duong, P. Renucci, B. L. Liu, C. Fontaine, T. Amand, D. Lagarde, and X. Marie, Phys. Rev. Lett. **107**, 136604 (2011).

[10] J. H. Jiang and M. W. Wu, Phys. Rev. B **79**, 125206 (2009).

[11] Y. Kato, R. C. Myers, A. C. Gossard, and D. D. Awschalom, Nature **427**, 50 (2004).

[12] Y. K. Kato, R. C. Myers, A. C. Gossard, and D. D. Awschalom, Phys. Rev. Lett. **93**, 176601 (2004).

[13] Y. K. Kato, R. C. Myers, A. C. Gossard, and D. D. Awschalom, Appl. Phys. Lett. **87**, 022503 (2005).

[14] L. Jiang and M. W. Wu, Phys. Rev. B **72**, 033311 (2005).

[15] S. A. Crooker and D. L. Smith, Phys. Rev. Lett. **94**, 236601 (2005).

[16] M. Beck, C. Metzner, S. Malzer, and G. H. Döhler, Europhys. Lett. **75**, 597 (2006).

[17] H. Knotz, A. W. Holleitner, J. Stephens, R. C. Myers, and D. D. Awschalom, Appl. Phys. Lett. **88**, 241918 (2006).

[18] D. J. English, P. G. Lagoudakis, R. T. Harley, P. S. Eldridge, J. Hübner, and M. Oestreich, Phys. Rev. B **84**, 155323 (2011).

[19] J. Rudolph, R. Hey, and P. V. Santos, Phys. Rev. Lett. **99**, 047602 (2007).

[20] G. E. Pikus, V. A. Marushchak, and A. N. Titkov, Sov. Phys. Semicond. **22**, 115 (1988).

[21] M. I. Dyakonov, V. A. Marushchak, V. I. Perel, M. N. Stepanova, and A. N. Titkov, Bull. Acad. Sci. USSR, Phys. Ser. **47**, 23 (1983).

[22] M. I. Dyakonov, V. A. Marushchak, V. I. Perel, and A. N. Titkov, Sov. Phys. JETP **63**, 655 (1986).

[23] V. I. Safarov and A. N. Titkov, Phys. B+C **117–118**, 497 (1983).

[24] H. Sanada, T. Sogawa, H. Gotoh, K. Onomitsu, M. Kohda, J. Nitta, and P. V. Santos, Phys. Rev. Lett. **106**, 216602 (2011).

[25] *Optical Orientation*, edited by F. Meier and B. P. Zakharchenya (North-Holland, Amsterdam, 1984).

[26] J. H. Buß, J. Rudolph, T. Schupp, D. J. As, K. Lischka, and D. Hägele, Appl. Phys. Lett. **97**, 062101 (2010).

[27] J. Rudolph, J. H. Buß, and D. Hägele, Phys. Status Solidi B **251**, 1850 (2014); J. H. Buß, A. Schaefer, T. Schupp, D. J. As, D. Hägele, and J. Rudolph, Appl. Phys. Lett. **105**, 182404 (2014).

[28] J. H. Buß, J. Rudolph, F. Natali, F. Semond, and D. Hägele, Appl. Phys. Lett. **95**, 192107 (2009).

[29] J. H. Buß, J. Rudolph, F. Natali, F. Semond, and D. Hägele, Phys. Rev. B **81**, 155216 (2010).

[30] J. H. Buß, J. Rudolph, S. Starosielec, A. Schaefer, F. Semond, Y. Cordier, A. D. Wieck, and D. Hägele, Phys. Rev. B **84**, 153202 (2011).

[31] S. Krishnamurthy, M. van Schilfgaarde, and N. Newman, Appl. Phys. Lett. **83**, 1761 (2003).

[32] O. Brandt, in *Group III Nitride Semiconductor Compounds*, edited by B. Gil (Clarendon Press, Oxford, 1998).

[33] R. M. Kemper, T. Schupp, M. Häberlen, T. Niendorf, H.-J. Maier, A. Dempewolf, F. Bertram, J. Christen, R. Kirste, A. Hoffmann, J. Lindner, and D. J. As, J. Appl. Phys. **110**, 123512 (2011).

[34] R. Klann, O. Brandt, H. Yang, H. T. Grahn, K. Ploog, and A. Trampert, Phys. Rev. B **52**, R11615 (1995).

[35] G. Bentoumi, A. Deneuville, E. Bustarret, B. Daudin, and G. Feuillet, Thin Solid Films **364**, 114 (2000).

[36] D. J. As, in *III-Nitride Semiconductor materials: Growth*, edited by M. O. Manasreh and I. T. Ferguson (Taylor and Francis, New York, 2003); D. J. As, S. Potthast, J. Schörmann, S. F. Li, K. Lischka, H. Nagasawa, and M. Abe, Mater. Sci. Forum **527**, 1489 (2006).

[37] We used the two-component epoxy UHU plus endfest 300 from UHU GmbH, Bühl, Germany. Special care was taken in proper glueing of the samples using a homemade press device to achieve thin, uniform epoxy layers. Almost no creep or drift was observed.

[38] Part No. PSt 150/5x5/7 from Piezomechanik Dr. Lutz Pickelmann GmbH, Munich, Germany.

[39] M. Shayegan, K. Karrai, Y. P. Shkolnikov, K. Vakili, E. P. D. Poortere, and S. Manus, Appl. Phys. Lett. **83**, 5235 (2003).

[40] Part No. SGD-1.5/120-LY11 from OMEGA Engineering, Stamford, Connecticut, USA.

[41] The strain values given refer to the average of the strain measured on the back of the piezo and on top of the sample.

[42] M. W. Bayerl, M. S. Brandt, T. Graf, O. Ambacher, J. A. Majewski, M. Stutzmann, D. J. As, and K. Lischka, Phys. Rev. B **63**, 165204 (2001).

[43] M. Fanciulli, T. Lei, and T. D. Moustakas, Phys. Rev. B **48**, 15144 (1993).

[44] C. Jagannath and R. L. Aggarwal, Phys. Rev. B **32**, 2243 (1985).

[45] M. Kriechbaum, R. Meisels, F. Kuchar, and E. Fantner, Phys. B+C **117–118**, 444 (1983).

[46] M. I. Dyakonov and V. I. Perel, Sov. Phys. Solid State **13**, 3023 (1972).

[47] M. W. Wu, J. H. Jiang, and M. Q. Weng, Phys. Rep. **493**, 61 (2010).

[48] G. Dresselhaus, Phys. Rev. **100**, 580 (1955).

[49] M. Cardona, V. A. Maruschak, and A. N. Titkov, Solid State Commun. **50**, 701 (1984).

[50] A. N. Chantis, M. Cardona, N. E. Christensen, D. L. Smith, M. van Schilfgaarde, T. Kotani, A. Svane, and R. C. Albers, Phys. Rev. B **78**, 075208 (2008).

[51] D. Hägele, S. Döhrmann, J. Rudolph, and M. Oestreich, Adv. Solid State Phys. **45**, 253 (2005).

[52] J. Fabian, A. Matos-Abiaguea, C. Ertlera, P. Stano, and I. Zutic, Acta Phys. Slovaca **57**, 565 (2007).

[53] R. Winkler, *Spin-Orbit Coupling Effects in Two-Dimensional Electron and Hole Systems* (Springer, Berlin, 2003).

[54] S. Döhrmann, D. Hägele, J. Rudolph, M. Bichler, D. Schuh, and M. Oestreich, Phys. Rev. Lett. **93**, 147405 (2004).

[55] Z. G. Yu, S. Krishnamurthy, M. van Schilfgaarde, and N. Newman, Phys. Rev. B **71**, 245312 (2005).

[56] K. Shen, J. Fu, and M. Wu, Solid State Commun. **151**, 1924 (2011).

[57] J. Y. Fu and M. W. Wu, J. Appl. Phys. **104**, 093712 (2008).

[58] M. Cardona, N. E. Christensen, and G. Fasol, Phys. Rev. B **38**, 1806 (1988).

[59] S. K. Pugh, D. J. Dugdale, S. Brand, and R. A. Abram, Semicond. Sci. Technol. **14**, 23 (1999).

[60] G. Ramírez-Flores, H. Navarro-Contreras, A. Lastras-Martínez, R. C. Powell, and J. E. Greene, Phys. Rev. B **50**, 8433 (1994).

[61] B. Pödör, Phys. Status Solidi B **16**, K167 (1966).

[62] R. L. Petritz and W. W. Scanlon, Phys. Rev. **97**, 1620 (1955).

[63] D. Chattopadhyay and H. J. Queisser, Rev. Mod. Phys. **53**, 745 (1981).

[64] P. H. Song and K. W. Kim, Phys. Rev. B **66**, 035207 (2002).

[65] J. Bardeen and W. Shockley, Phys. Rev. **80**, 72 (1950).

[66] D. J. As, D. Schikora, A. Greiner, M. Lübbers, J. Mimkes, and K. Lischka, Phys. Rev. B **54**, R11118 (1996).

[67] M. Kohno, T. Nakamura, T. Kataoka, R. Katayama, and K. Onabe, Phys. Status Solidi C **5**, 1805 (2008); J. N. Kuznia, J. W. Yang, Q. C. Chen, S. Krishnankutty, M. A. Khan, T. George, and J. Frietas, Appl. Phys. Lett. **65**, 2407 (1994); H. Okumura, S. Misawa, T. Okahisa, and S. Yoshida, J. Cryst. Growth **136**, 361 (1994); S. V. Novikov, N. M. Stanton, R. P. Campion, R. D. Morris, H. L. Geen, C. T. Foxon, and A. J. Kent, Semicond. Sci. Technol. **23**, 015018 (2008).

[68] D. J. As, T. F. D., Schikora, K. Lischka, V. Cimalla, J. Pezoldt, R. Goldhahn, S. Kaiser, and W. Gebhardt, Appl. Phys. Lett. **76**, 1686 (2000).

[69] D. J. As and K. Lischka, in *Nonpolar Cubic III-Nitrides: From the Basics of Growth to Device Applications*, edited by M. Henini (Elsevier, Oxford, 2013).

[70] D. Jena, Phys. Rev. B **70**, 245203 (2004).

[71] Here we corrected for several misprints in the English version of the corresponding section of Ref. 25, including the correct value of γ_3^{pop} and inconsistent use of γ_3.

[72] We used the values $\gamma_e = 0.84$ eV Å^3, $n_{\mathrm{Disl}} = 1 \times 10^{10}\,\mathrm{cm}^{-2}$ for sample A and $n_{\mathrm{Disl}} = 2 \times 10^9\ \mathrm{cm}^{-2}$ for sample B, respectively, as well as

$\mu_{\mathrm{pop}}^{\mathrm{sim}} = 320\,\mathrm{cm}^2/\mathrm{Vs}$ and $\mu_{\mathrm{disl}}^{\mathrm{sim}} = 120\,\mathrm{cm}^2/\mathrm{Vs}$ for sample A and $\mu_{\mathrm{disl}}^{\mathrm{sim}} = 790\,\mathrm{cm}^2/\mathrm{Vs}$ for sample B, respectively, for the calculation of γ_s^{D}.

[73] V. I. Melnikov and E. I. Rashba, Sov. Phys. JETP **34**, 1353 (1972).

[74] E. Y. Sherman, Appl. Phys. Lett. **82**, 209 (2003).

[75] R. J. Elliott, Phys. Rev. **96**, 266 (1954).

[76] G. L. Bir, A. G. Aronov, and G. E. Pikus, Sov. Phys. JETP **42**, 705 (1976).

[77] G. Wang, C. R. Zhu, B. L. Liu, H. Ye, A. Balocchi, T. Amand, B. Urbaszek, H. Yang, and X. Marie, Phys. Rev. B **90**, 121202 (2014).

[78] J. H. Buß, J. Rudolph, S. Shvarkov, H. Hardtdegen, A. D. Wieck, and D. Hägele, Appl. Phys. Lett. **102**, 192102 (2013).